THE JOURNAL OF PHYSICAL CHEMISTRY C

ARTICLE

pubs.acs.org/JPCC

An Investigation of the Behavior of Completely Siliceous Zeolite ZSM-5 under High External Pressures

Yueqiao Fu, Yang Song,* and Yining Huang*

Department of Chemistry, The University of Western Ontario, London, Ontario, Canada

Supporting Information

ABSTRACT: The behavior of completely siliceous zeolite ZSM-5 (Si-ZSM-5) under high pressures up to 16 GPa were investigated by in situ Raman spectroscopy and X-ray diffraction with synchrotron radiation in a diamond anvil cell. Pressure-induced amorphization was observed in both as-made and calcined Si-ZSM-5, which transform to a low-density amorphous silica first and then to a high-density amorphous silica. However, transition pressures and reversibility were different for as-made and calcined Si-ZSM-5. It was found that the existence of the template molecules occluded in the zeolite framework is mainly responsible for these differences.

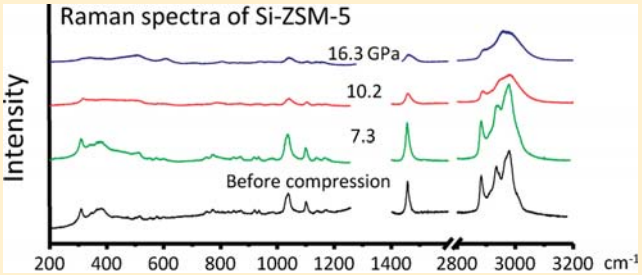

INTRODUCTION

Zeolites are microporous aluminosilicates with well-defined channels and cavities.[1] They have been widely used as ion-exchangers, molecular sieves, sorbents, and catalysts.[2] The stability of zeolites is crucial to their applications. Many experimental and theoretical studies have been concentrated on their thermal stability.[3] On the contrary, their behavior under external high pressures has received less attention. Only a handful of the zeolite topologies have been studied under high pressures.[4−13] Much of the early work has been focused on (1) the pressure-induced structural transformations between crystalline phases;[14] (2) pressure-induced hydration and the compressibility of zeolites affected by nonframework species;[15] (3) the effect of pressure on ionic conductivity of zeolites;[16] and (4) pressure-induced amorphization (PIA) and the reversibility of this process upon decompression.[17]

Initially discovered in hexagonal ice,[18] PIA has been the subject of many studies[8,19−21] and found to occur in various materials. Pressure-induced amorphous state appears to be a universal property of condensed materials.[22] The PIA in zeolitic systems has been investigated experimentally and theoretically in the past decade.[8,19,20,23−26] Pressure-induced amorphous phases of several zeolites can partially or totally revert back to the initial zeolite's crystalline structure upon decompression. The recent work by Greaves and co-workers[10,21,27,28] has shown that upon compression a zeolite may transform to two different amorphous phases: (1) a low-density amorphous (LDA) phase, which is a so-called "perfect glass" with relatively ordered structure and negligible configuration entropy, and (2) a high-density amorphous (HDA) phase with a normal density of aluminosilicate glass. This phenomenon of the occurrance of more than one amorphous phase with the same chemical composition but different densities and entropies is called polyamorphism.[29] Usually, the topology of the material in the crystalline phase is preserved in the LDA phase, but lost in the HDA phase.[30−32]

Zeolite ZSM-5 is a representative member of a class of high-silica zeolites with applications in adsorption, catalysis,[33−35] and thin films/membranes.[36,37] It is often used as a model system for zeolite property study.[38] ZSM-5 consisting of 4-, 5-, 6-, and 10-membered rings has a framework with two interconnected channel systems: sinusoidal 10-memebred ring (10-MR) channels along the [100] direction, interconnected with straight 10-MR channels that run parallel to the [010] direction (Figure 1). A tortuous pore path is present in the [001] direction.[39] The three-letter code for this topology assigned by the International Zeolite Association is MFI. ZSM-5 is usually synthesized in the presence of tetrapropylammonium cations (TPA^+), and the template ions are found in the intersections of the two channel systems.[40]

Completely siliceous ZSM-5 (Si-ZSM-5) is also known as silicalite-1. Its framework is neutral and hydrophobic. The behavior of Si-ZSM-5 under pressures was first investigated by Liu et al.[41] They suggested that the Si-ZSM-5 irreversibly transforms into zeolite ZSM-11 at 4 GPa. Since the study did not use any in situ technique, no information on the structure change during the compression/decompression is available. More recently,

Special Issue: Chemistry and Materials Science at High Pressures Symposium

Received: May 31, 2011
Revised: August 13, 2011
Published: September 02, 2011

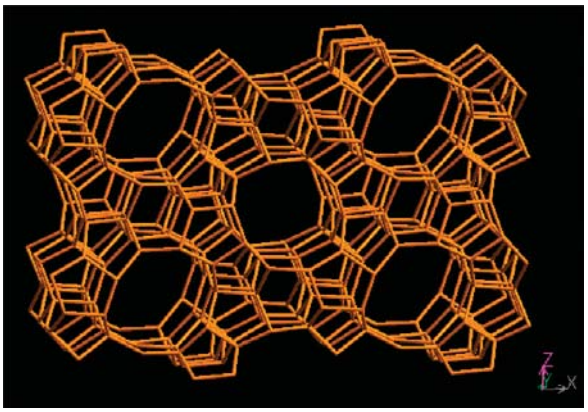

Figure 1. Zeolite structure of ZSM-5 viewed along the [010] direction.

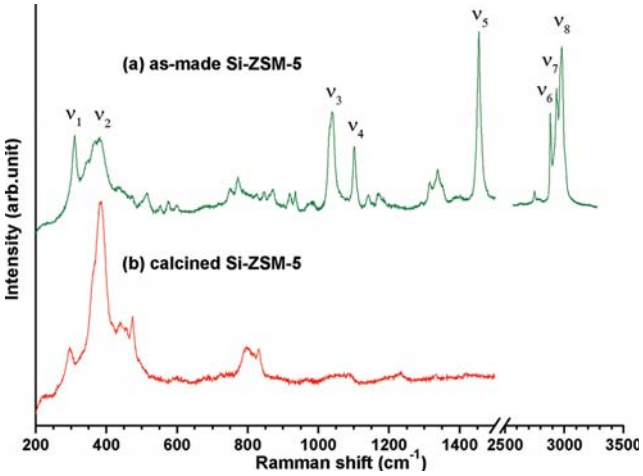

Figure 2. Raman spectra of as-made (a) and calcined (b) Si-ZSM-5 at ambient conditions.

the work by Haines and co-workers investigated the possibility of using siliceous ZSM-5 synthesized in fluoride medium as a precursor to prepare dense silica glass under high pressures.[42] The same authors also studied the PIA of silicalite-1 under high pressure with insertion of guest species. Silicalite-1 loaded with CO_2 is stable up to 22 GPa, but without the guest species, Si-ZSM-5 transforms into an amorphous material completely at 8 GPa.[43]

Therefore, the studies and understanding of the high-pressure behavior of ZSM-5 under the influence of other factors remain highly relevant in further development of its catalytic and storage functionalities. In complement to all previous high-pressure studies on ZSM-5, especially those by Haines,[42,43] here we report a comparative study between as-made and calcined ZSM-5 using comprehensive structural characterization techniques. The main objective of the present work is to study the behavior of Si-ZSM-5 with and without template cations (TPA^+) under high pressures. Particular attention is focused on (1) the differences in reversibility of the amorphization between the Si-ZSM-5 samples with and without TPA^+ and (2) the role of the encapsulated organic molecules in framework transformation under high pressures.

EXPERIMENTAL SECTION

As-made Si-ZSM-5 was prepared by hydrothermal synthesis method using tetrapropylammonium bromide (TPAB) as a template.[44] The calcined Si-ZSM-5 was obtained by heating the as-made sample in a Muffle furnace at 550 °C for 3 h to remove the template molecules. The identity, crystallinity, and purity of the samples were checked by powder X-ray diffraction (XRD).

The high-pressure experiments were performed with symmetric diamond anvil cells (DACs), which have a pair of type I diamonds with a 600 μm culet. A hole with a diameter of 200 μm was drilled in the center of "pre-indented" stainless steel gaskets and used as a sample chamber. A ruby (Cr^{3+}-doped α-Al_2O_3) chip was added in the sample chamber as a pressure calibrant, and the pressure was determined from the well-established ruby R_1 fluorescence line shift. Since the behavior of a zeolite under pressure depends on the type of pressure-transmitting medium (PTM) being used (penetrating or nonpenetrating PTM[4,45,46]), all high-pressure experiments we performed were without PTM in order to study the pure pressure effect by avoiding any possible interactions between the sample and the PTM that may enter the channels of the sample during compression. In addition, even without PTM, in the pressure region where most materials remain crystalline (e.g., < 5 GPa), no significant nonhydrostatic effect was observed from the ruby fluorescence profile.

Upon loading the sample, in situ Raman spectra were obtained using a customized Raman microspectroscopy system. A 488 nm line from an Innova Ar^+ laser (Coherent, Inc.) was used as the excitation source and was focused to less than 5 μm on the sample by an Olympus microscope. The Rayleigh line was blocked using a pair of notch filters. The scattered light was dispersed using an imaging spectrograph equipped with an 1800 lines/mm grating, achieving a best resolution of 1 cm^{-1} when the entrance slit is set to 10 μm, as indicated by the full-width-at-half-maximum of neon lines. The scattered light was then recorded using an ultrasensitive liquid nitrogen-cooled, back-illuminated charge-coupled device (CCD) detector made by Princeton Instruments. The spectrometer was calibrated using standard neon lines with an uncertainty of ±1 cm^{-1}. A minimum of 15 min was allowed to ensure equilibrium in the cell upon increasing or decreasing of the pressure. At each pressure, the Raman spectrum of the sample was collected for 1 min, and the average laser power on the sample was maintained at ~30 mW. To avoid the strong first-order Raman mode of the diamond at 1334 cm^{-1}, the spectra were collected in several regions of 200−1200, 1440−1600 and 2800−3200 cm^{-1}. All Raman measurements were conducted at room temperature.

Angle-dispersive X-ray diffraction (ADXRD) experiments were carried out at an insertion device undulator beamline (16ID-B) at the High Pressure Collaborative Access Team (HPCAT), Advanced Photon Source (APS), Argonne National Laboratory (ANL). A monochromatic X-ray beam with wavelength of 0.369126 Å and a MAR165 CCD X-ray detector were used to obtain the two-dimensional (2D) Debye−Scherrer diffraction patterns. The 2D patterns were then converted to one-dimensional diffraction patterns using FIT2D software.

Scanning electron microscopy (SEM) was used to examine the morphology of the initial and recovered samples. The recovered samples in the gaskets were carefully removed from the DAC after decompression and imaged by SEM using a Leo/Zesis 1540XB FIB/SEM Crossbeam.

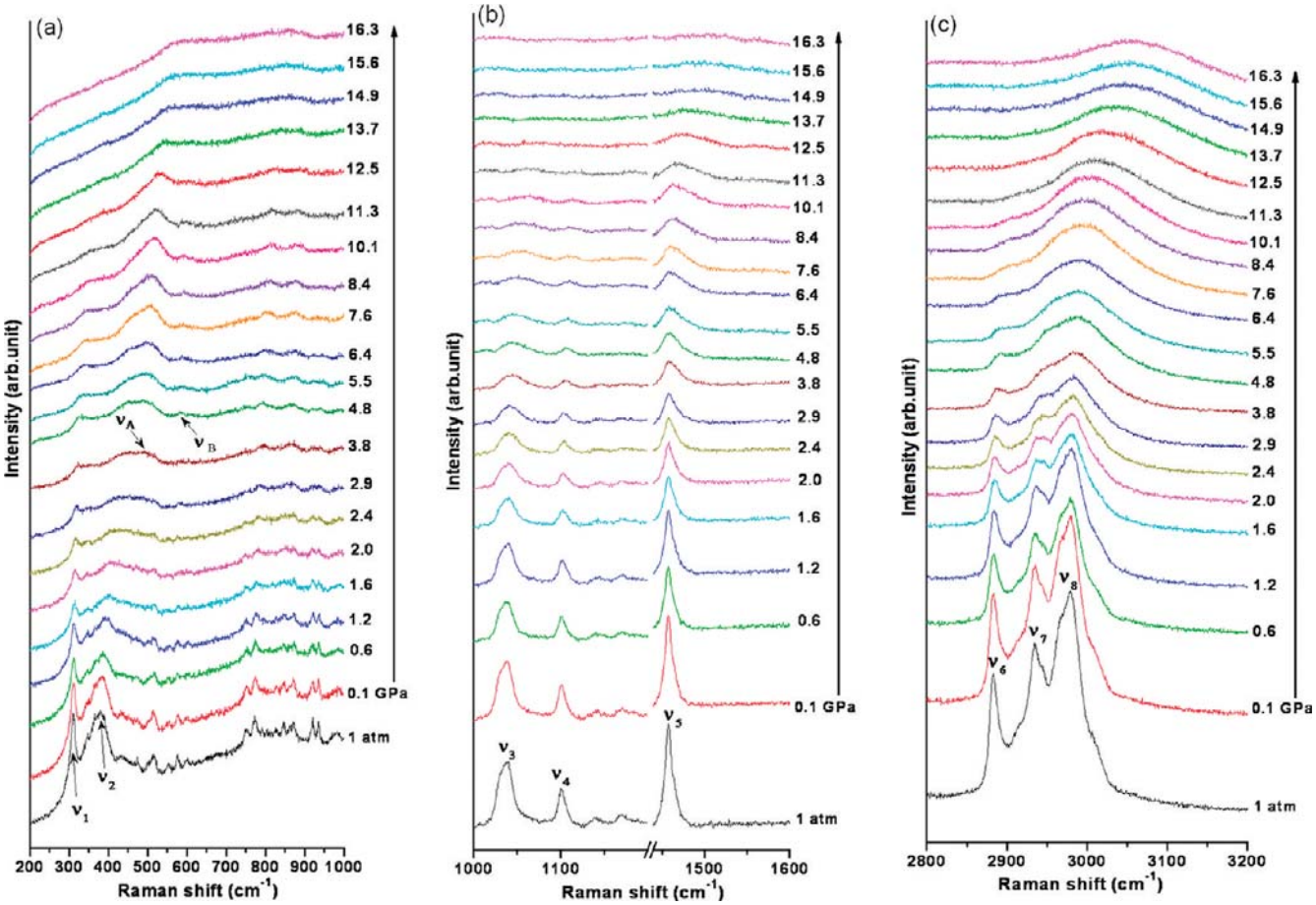

Figure 3. Selected Raman spectra of as-made Si-ZSM-5 on compression in the pressure region 0−16.3 GPa in the spectral regions of 200−1000 cm^{-1}- (a), 1000−1600 cm^{-1}(b), and 2800−3200 cm^{-1} (c). The vertical arrow indicates the experimental sequence.

RESULTS AND DISCUSSION

Completely Siliceous ZSM-5 with Template (As-Made Si-ZSM-5). *Raman Spectra upon Compression.* Raman spectroscopy was used to monitor the effect of pressure on the structure of Si-ZSM-5. The Raman spectrum of as-made Si-ZSM-5 at ambient conditions (Figure 2a) is consistent with those reported previously.[47,48] The band labeled ν_2 belongs to the zeolite framework due to the Si−O−Si bending vibrations, and the rest of the bands originate from the occluded TPA$^+$ cations. The detailed assignments are given in the Supporting Information Table S1. The in situ Raman spectra of the as-made Si-ZSM-5 were acquired as a function of pressure up to 16.3 GPa at room temperature. The selected spectra are shown in Figure 3. Based on the appearance, the spectra can be broadly divided into three regions.

Below 2.9 GPa, only the peaks belonging to as-made Si-ZSM-5 are observed. The fact that no new peak appears implies that no new phase occurs below 2.9 GPa. However, Figure 3a shows that the ν_2 band due to zeolitic framework vibration is gradually broadened, suggesting that the framework of as-made Si-ZSM-5 does undergo deformation with increasing pressure. The strong bands (ν_3−ν_8) in Figure 3b,c are due to the template (TPA$^+$) trapped at the channel intersections. These bands do not change significantly with increasing pressure, which indirectly confirms that the framework of as-made Si-ZSM-5 mainly remains intact. However, a careful inspection of the spectra reveals that these bands do experience a slight line-broadening with increasing pressure, indicating that the template molecules experience a slight change in their environment (which is the surrounding zeolite framework) resulting from the slight deformation of the zeolite framework.

Between 3 and 7.6 GPa, a broad new band (labeled ν_A) appears. This new peak begins to emerge at 491 cm^{-1} at 3.8 GPa. At 4.8 GPa, a second new broad band (ν_B) shows up at 588 cm^{-1}. The appearance of these new bands is indicative of the formation of an amorphous phase at about 3 GPa, suggesting that PIA begins. The intensity of the ν_A band increases with increasing pressure, which is accompanied by the gradual disappearance of the ν_2 band due to the zeolite framework. At 7.6 GPa, the ν_A band becomes the most prominent peak, and the zeolitic peak is almost invisible. In this pressure range, the intensities of all the bands due to TPA$^+$ gradually decrease, and the peaks gradually become very broad. These observations indicate that there is a dramatic change in the environment of template molecules. The initially ordered arrangement of the TPA$^+$ cations in the zeolite has become highly disordered. It seems that, starting at around 3 GPa, as-made Si-ZSM-5 has partially transformed into an amorphous phase. Both the zeolite and amorphous silica coexist between 3 and 7.6 GPa with the amount of amorphous silica increasing with increasing pressure.

Above 7.6 GPa, the ν_2 mode is no longer visible, which means the framework of as-made Si-ZSM-5 collapses completely. All the bands due to the template become remarkably broad, and they almost disappear in the baseline above 13.7 GPa, indicating completely disordered orientations of the template cations. Above 7.6 GPa, the intensities of the two new bands (ν_A and ν_B) belonging to the amorphous material also decrease gradually.

The pressure dependences of characteristic Raman bands in the region of 200−1000 cm^{-1} during compression are shown in Figure 4, where all the bands exhibit a blue shift. In general, the change in the slope of pressure-dependence, disappearance of the initial peaks, and appearance of new peaks provide evidence for the start and finish of phase transitions including amorphization. The approximate phase boundaries for as-made Si-ZSM-5 are indicated in Figure 4. The first distinct region is between 0 and 2.9 GPa where the Raman bands, ν_1 and ν_2, show linear and positive pressure dependences with $d\nu/dP$ values of 2.34 and 14.48 cm^{-1}/GPa, respectively. The values indicate that the framework of the zeolite is more compressible than that of the template ions. In this region, the solid is mainly as-made Si-ZSM-5, whose structure gradually deforms under pressures. In the second pressure region (3−7.6 GPa), the ν_2 band shows a much smaller $d\nu/dP$ value (1.87 cm^{-1}/GPa) than that in the low-pressure region, and two new bands (ν_A and ν_B) start appearing, indicating that an amorphous material forms in the sample. In this pressure range, the crystalline zeolite gradually transforms to an amorphous phase under pressure, and the system is a mixture of both. In the third region (above 7.6 GPa), the ν_2 band disappears, and the bands assigned to the amorphous material both show larger $d\nu/dP$ values than those in the second pressure region, which may imply the formation of a second amorphous phase. Overall, the two phase boundaries indicate the crystalline-to-amorphous and the amorphous-to-amorphous phase transitions, respectively.

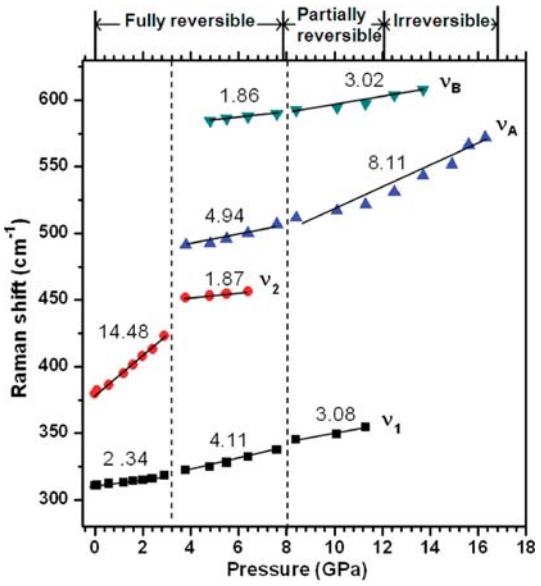

Figure 4. Pressure dependences of the Raman shift of selected modes for as-made Si-ZSM-5. The vertical dashed lines denote the proposed phase boundaries. The $d\nu/dP$ values (cm^{-1}/GPa) are indicated. Regions labeled on the top of the figure indicate the reversibility of PIA of the as-made Si-ZSM-5.

Raman Spectra upon Decompression. The reversibility of the pressure effect on zeolite structure was studied. Raman spectra upon successive decompression of the pressurized as-made Si-ZSM-5 were collected until ambient pressure was reached (Figure 5a). The profiles of the new Raman bands (ν_A and ν_B) due to an amorphous material forming at high-pressure gradually change with decreasing pressure (Figure 5a). In the decompression spectra, a new weak band (ν_C) was observed at above 800 cm^{-1}. This band attributed to the amorphous material is hardly seen in the compression spectra. All three amorphous bands shift to lower frequencies and gain intensity with decreasing pressure.

The fact that the spectra above 400 cm^{-1} taken at ambient conditions before compression and after decompression look very different (Figure 5a) implies that the amorphous phase is mostly retained after releasing pressure. The spectrum of the retrieved sample above 400 cm^{-1} has three peaks, and their

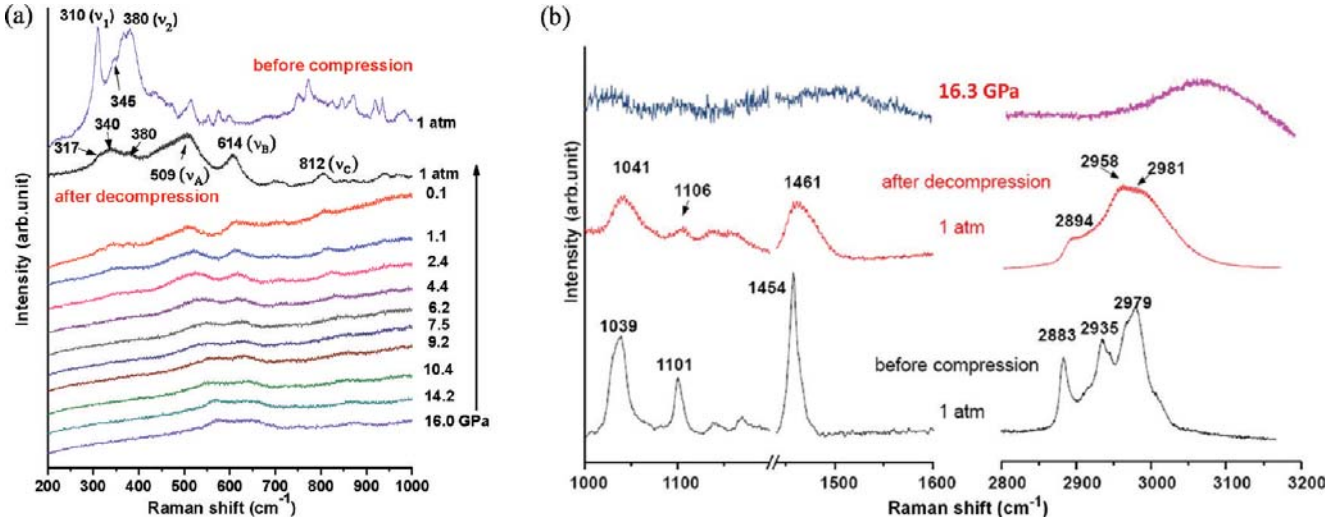

Figure 5. (a) Selected Raman spectra of as-made Si-ZSM-5 during decompression from 16.0 GPa to ambient pressure in the spectral region of 200−1000 cm^{-1}. The vertical arrow indicates the experimental sequence. (b). Raman spectra of as-made Si-ZSM-5 before compression, compressed to 16.3 GPa and after decompression in the spectral regions of 1000−1600 and 2800−3200 cm^{-1}.

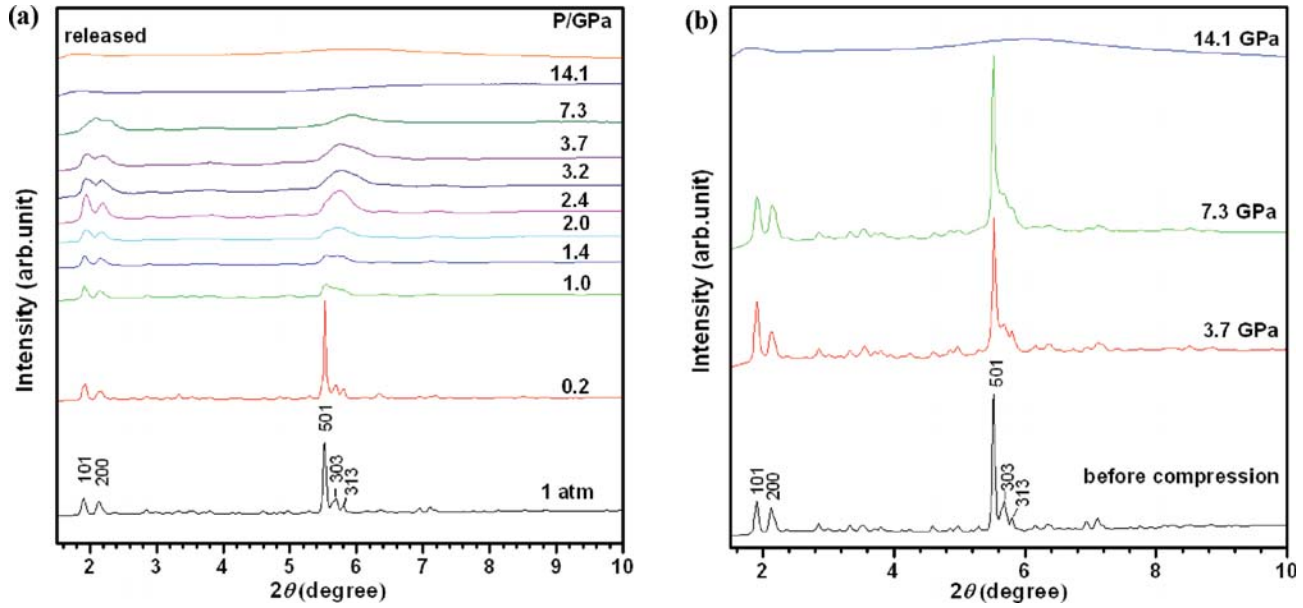

Figure 6. XRD patterns of as-made Si-ZSM-5 during compression and the pattern of the sample recovered from 14.1 GPa (a) and those recovered from different high-pressure runs (maximum pressures are labeled) (b) at room temperature using the wavelength of 0.369126 Å. Miller indices of the relatively strong reflections are labeled on the 1 atm pattern.

positions are at 509, 614, and 812 cm^{-1} for ν_A, ν_B, and ν_C, respectively. Previous studies[49−51] have shown that the high-pressure treatment converts an LDA silica with 5- and 6-MRs[52] irreversibly to an HDA silica with mainly 3- and 4-MRs.[53] The Raman spectrum of recovered HDA silica has three bands at 500, 610, and 800 cm^{-1}, and its spectral appearance is very similar to the spectrum of decompressed as-made Si-ZSM-5 in the region of 400−1000 cm^{-1}. Since the siliceous ZSM-5 framework studied in this work merely consists of silicon and oxygen atoms, it is reasonable to conjecture that high-pressure treatment of as-made Si-ZSM-5 also leads to the formation of two amorphous phases. First, the Si-ZSM-5 starts transforming to the LDA silica at around 3 GPa, and the degree of the conversion to the LDA silica increases with increasing pressure. Second, the LDA silica starts to evolve into the HDA silica at around 7 GPa, with the amount of the HDA silica gradually increasing with increasing pressure. At very high pressure of around 14 GPa, only the HDA silica exists in the system.

When the pressure is decreased to 2.4 GPa, a weak broad hump appears in the region of 330−400 cm^{-1} (Figure 5a). This broad envelop comprising several overlapping bands becomes more distinct with further lowering pressure. For the recovered sample, three overlapping peaks below 400 cm^{-1} (317, 340, and 380 cm^{-1}) exhibit some similarities to those (ν_1 and ν_2) in the spectrum of the sample before compression. The band at 380 cm^{-1} of the recovered sample is likely associated with the Si-ZSM-5 framework. Since the recovered sample is X-ray amorphous (see discussion below), the Raman data suggest that for a small portion of the recovered sample, the MFI topology (i.e., the Si−O−Si connectivity) is re-established, although long-range ordering is still lacking.

Figure 5b compares the Raman spectra above 1000 cm^{-1} of the TPA^+ cations occluded in as-made Si-ZSM-5 before and after high-pressure treatment. Upon releasing pressure, the template peaks disappeared and at high pressure reappear. However, the spectrum taken at ambient conditions after decompression shows that the template peaks remain very broad compared to the corresponding bands before compression, and the peak positions are not identical. These results imply that the environments of the trapped template cations are still very disordered, indicating that the recovered sample still remains amorphous.

The Behavior of Crystalline TPAB Solids under High Pressure. To better understand the behavior of the template molecule occluded in the Si-ZSM-5 framework, an in situ Raman study of pure crystalline TPAB solids was carried out in the pressure range of 0−16 GPa. The behavior of TPAB solids under pressure was examined before, but the highest pressure was only 4 GPa.[54] Figure S1 illustrates the spectra of TPAB as a function of pressure upon compression. In the pressure range of 0−4.2 GPa, all the bands gradually shift to higher energies. Above 5.1 GPa, the intensities of all the bands decrease dramatically, which suggests the start of PIA resulting from conformational and positional disordering. Between 5.8 and 11.0 GPa, all the peaks gradually become extremely broad with very low intensity. They almost disappear into the baseline at 11.0 GPa, implying that the solid is completely disordered with each cation having its own local environment and the TPA^+ cations adopting all the possible orientations. There must also be distributions of bond angle and distance for the TPA^+ ion. No further change in spectra is observed beyond this pressure, which suggests that the PIA is complete at 11.0 GPa.

Figure S2 show the evolution of the Raman spectra of crystalline TPAB upon decompression from 16.1 GPa. No drastic change was detected until 2.2 GPa, except that the broad humps gradually shift to lower frequencies with increasing intensities. At 0.4 GPa, the broad peaks suddenly become very sharp and very well resolved. Although there is a hysteresis, the spectrum of the recovered sample is almost identical to that of the TPAB before compression, i.e., the peak positions and line-widths are identical. Thus, the changes in the spectra induced by pressure are completely reversible upon decompression. It seems that the TPA^+ cations, which are in a completely disordered state, return to the ordered arrangement in their initial crystalline state after pressure is released, clearly indicating that the PIA of crystalline TPAB is totally reversible. The ambient spectrum of pure TPAB

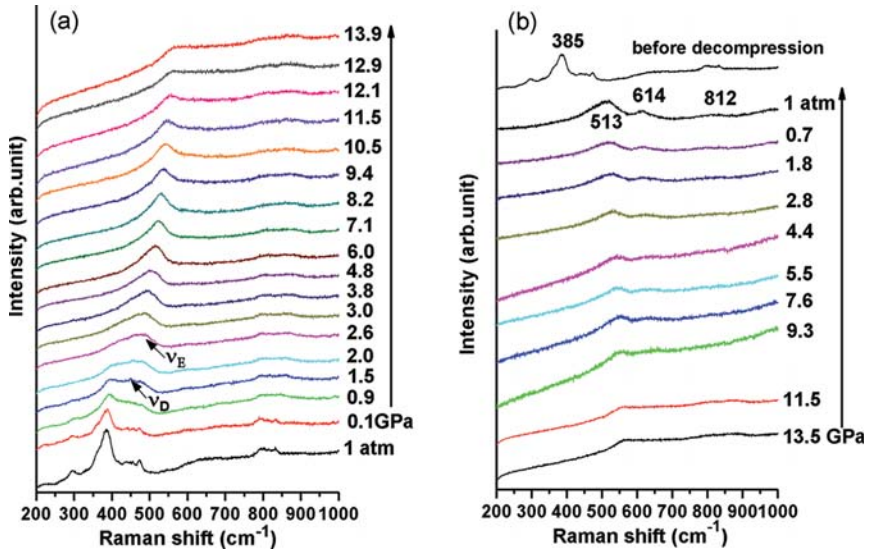

Figure 7. Selected Raman spectra of calcined Si-ZSM-5 on compression (a) and decompression (b) in the pressure region 0−13.9 GPa in the spectral region of 200−1000 cm^{-1}. The vertical arrow indicates the experimental sequence.

solid recovered from 16.1 GPa is much different from that of the TPA^+ in the as-made Si-ZSM-5 sample obtained from decompression from 16 GPa (Figure 5b). The difference is due to the fact that the TPA^+ environment in the recovered as-made Si-ZSM-5 sample (i.e., the HDA silica) remains disordered.

Powder XRD Patterns. Powder XRD was used to gain direct information on pressure-induced structural transformations. The selected XRD patterns of as-made Si-ZSM-5 acquired upon compression are shown in Figure 6a. The sharp reflections indexed as (*501*), (*303*), (*313*) (*101*), and (*200*) observed at ambient conditions become significantly weaker and broader above 1.0 GPa. At 7.3 GPa, although very weak and broad, the three major reflections, (*101*), (*200*), and (*501*), of as-made Si-ZSM-5 remain identifiable, suggesting that at this pressure, at least part of the sample still has MFI topology. The sample becomes completely amorphous at 14.1 GPa. After decompression to ambient conditions, the pattern of the released sample looks identical to that of the sample compressed at 14.1 GPa without reappearance of the MFI reflections, suggesting that the recovered sample remains largely X-ray amorphous.

The XRD data suggest that after compressing as-made Si-ZSM-5 at 14.1 GPa, the zeolite loses its long-range ordering permanently. However, as mentioned earlier, the Raman spectrum of the recovered sample shows not only the peaks belonging to the HDA silica, but also the signature band due to the MFI topology. The Raman and XRD results are not inconsistent with each other. Raman spectroscopy probes short-range ordering in solids, and XRD is sensitive to long-range ordering. The XRD data show that the HDA silica formed by compressing the zeolite to 14 GPa remains X-ray amorphous at ambient conditions, whereas the Raman spectrum further indicates that a small portion of the HDA appears to transform back to the LDA phase where the Si−O−Si connectivity (i.e., the short-range ordering) is similar to MFI topology, but the long-range ordering is still lacking.

Calcined (Template-Free) Si-ZSM-5. *Raman Spectra on Compression.* The ambient spectrum of calcined Si-ZSM-5 (Figure 2b) is consistent with that reported by Dutta et al.[55] The most prominent band at 385 cm^{-1} is assigned to the Si−O−Si bending vibrations of the 5-MRs, and it is the only peak that can be followed at high pressures. The weak bands near 500 cm^{-1} are attributed to the Si−O−Si bending vibrations of the 4- and 6-MRs and the band at around 830 cm^{-1} is assigned to the Si−O stretching vibration.[55]

The calcined Si-ZSM-5 was compressed to 13.9 GPa at room temperature, and the selected Raman spectra are shown in Figure 7a. The strongest band (at 385 cm^{-1}) is gradually suppressed beyond 0.9 GPa. After 1.5 GPa, two new weak bands (ν_D and ν_E) appear at 450 and 481 cm^{-1} on the high-frequency side of the main zeolite peak. The new bands are similar to those of the LDA silica mentioned before.[56,57] These observations show that the framework of calcined Si-ZSM-5 is quickly distorted under high pressure, and an amorphous material (the low-density silica) forms quickly. Above 3.0 GPa, the ν_E band is the only band in the spectra, and gradually shifts to higher frequencies with increasing pressure. In the meantime, the zeolite band disappears completely, which implies that the crystalline Si-ZSM-5 becomes completely amorphous. Above 11.5 GPa, the ν_E band gradually weakens with increasing pressure.

Raman Spectra on Decompression. The Raman spectra of the calcined Si-ZSM-5 on decompression are shown in Figure 7b from 13.5 GPa to ambient pressure. The new band ν_E gradually shifts to lower frequency and is retained at ambient pressure. Two additional bands appear gradually during decompression and are clearly visible at 614 and 812 cm^{-1} in the spectrum of ambient pressure. The initial Raman bands due to the zeolite did not reappear at all, which means the framework of the calcined Si-ZSM-5 has totally collapsed and the PIA is irreversible. The spectrum of the recovered sample looks the same as that of the HDA silica obtained by high-pressure treatment of the LDA silica in the previous studies.[49−51]

The combination of compression and decompression Raman data indicates that calcined Si-ZSM-5 quickly deforms under pressure and starts to form the LDA silica at around 1.5 GPa. Between 1.5 and 3 GPa, the zeolite continues to transform to the LDA silica with increasing pressure. The LDA silica starts to evolve into the HDA silica at around 3 GPa. Only the HDA silica exists in the system at 11 GPa and beyond.

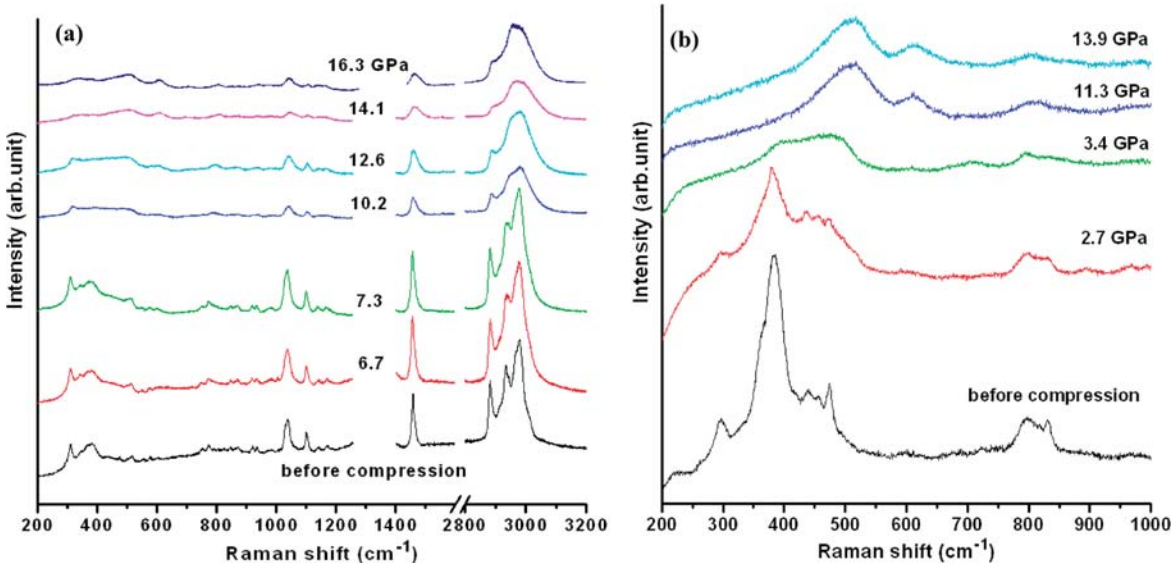

Figure 8. Raman spectra of as-made (a) and calcined (b) Si-ZSM-5 samples recovered from different high-pressure runs (maximum pressures are labeled) compared with the spectrum of the sample before compression.

Comparison of the Behavior of As-Made and Calcined Si-ZSM-5 under High Pressures and Their Reversibility of PIA. The spectra of as-made and calcined Si-ZSM-5 recovered from compression to 14 GPa or higher look very similar in the region above 500 cm^{-1} and strongly resemble those of the HDA silica reported in the literature. This indicates that both zeolites are converted to the HDA silica at high pressures. However, for as-made Si-ZSM-5, the band at around 380 cm^{-1} attributed to the ZSM-5 framework seen in the spectrum of the initial uncompressed sample reappears as a broad, weak shoulder after decompression from 16 GPa. These observations suggest that, although most of the compressed as-made Si-ZSM-5 sample remains as the HDA phase upon decompression, a small amount of the HDA silica does transform back to the LDA where MFI topology is re-established. In contrast, the HDA phase obtained by compression of calcined Si-ZSM-5, which has no TPA^+ cations, is completely preserved upon releasing pressure. Apparently, the template molecules play a key role in partially restoring the MFI connectivity when the pressure is released. The existence of the occluded TPA^+ cations facilitates the partial restoration of the MFI connectivity because the interaction between the TPA^+ and zeolite framework preserves some silicate fragments with key local structures associated with the MFI topology, and these key structural fragments exist even at 16.3 GPa. Upon releasing pressure, the TPA^+ cations redirect these silicate species with MFI signature to partially reform the MFI topology. A similar situation has been found in clathrasil dodecasil-3R with organic molecules (amino-adamantane) in its cages in a previous study.[5]

Previous work showed that PIA can be reversible or partially reversible in some systems,[17,19,22] i.e., the amorphous phase may revert back to its original crystalline state when the pressure is released. There exists a threshold pressure.[24,58] Below this pressure PIA is completely reversible, and above this pressure PIA is not reversible. In order to determine whether such a threshold pressure exists in as-made and calcined Si-ZSM-5, we examined the reversibility of amorphization in these zeolites. Specifically, we characterized the recovered samples obtained by first compressing the zeolite to desired pressures and then releasing them to the ambient value. Raman spectra of the samples recovered from the as-made Si-ZSM-5 compressed to the different pressures are shown in Figure 8a. The spectra of the samples recovered from compression to 7 GPa or less look identical to that of as-made Si-ZSM-5 without compression. As mentioned before, 7 GPa is the approximate pressure at which the LDA silica is just about to transform to the HDA phase. The Raman data suggest that the PIA in as-made Si-ZSM-5 is totally reversible from the LDA phase, i.e., the LDA silica formed from as-made Si-ZSM-5 can completely transform back to the crystalline MFI structure as long as the maximum pressure applied is 7 GPa or less. The spectra of the samples recovered from 10.2 and 12.6 GPa are similar: all the TPA^+ peaks show a decrease in the intensity and an increase in the line-width. The peak due to the zeolite at 385 cm^{-1} becomes extremely broad. These phenomena indicate that a large part of the recovered sample remains amorphous. Thus, the PIA in as-made Si-ZSM-5 appears to be only partially reversible in the pressure range between 7.3 and 12.6 GPa. The spectra of the samples retrieved from 14.1 and 16.3 GPa are the same, the bands due to the HDA silica are seen clearly, and the original bands due to the zeolite become extremely broad, suggesting that the recovered sample is highly amorphous only with a very small amount of the material regaining the MFI topology.

XRD is also used to determine the reversibility of the sample. The XRD patterns of the recovered as-made Si-ZSM-5 samples from different high-pressure runs are compared with the pattern of the sample before compression (Figure 6b). The patterns of the recovered sample treated at 3.7 and 7.3 GPa look identical to that of the uncompressed as-made Si-ZSM-5, confirming that the PIA is completely reversible and the long-range ordering of the initial zeolite is recovered completely. This result is consistent with the Raman data. The pattern of the sample recovered from the treatment at the highest pressure (14.1 GPa) only exhibits a extremely weak and broad envelop, suggesting that after the treatment at this pressure, the sample is completely amorphous, no crystalline structure is recovered, and the PIA is irreversible.

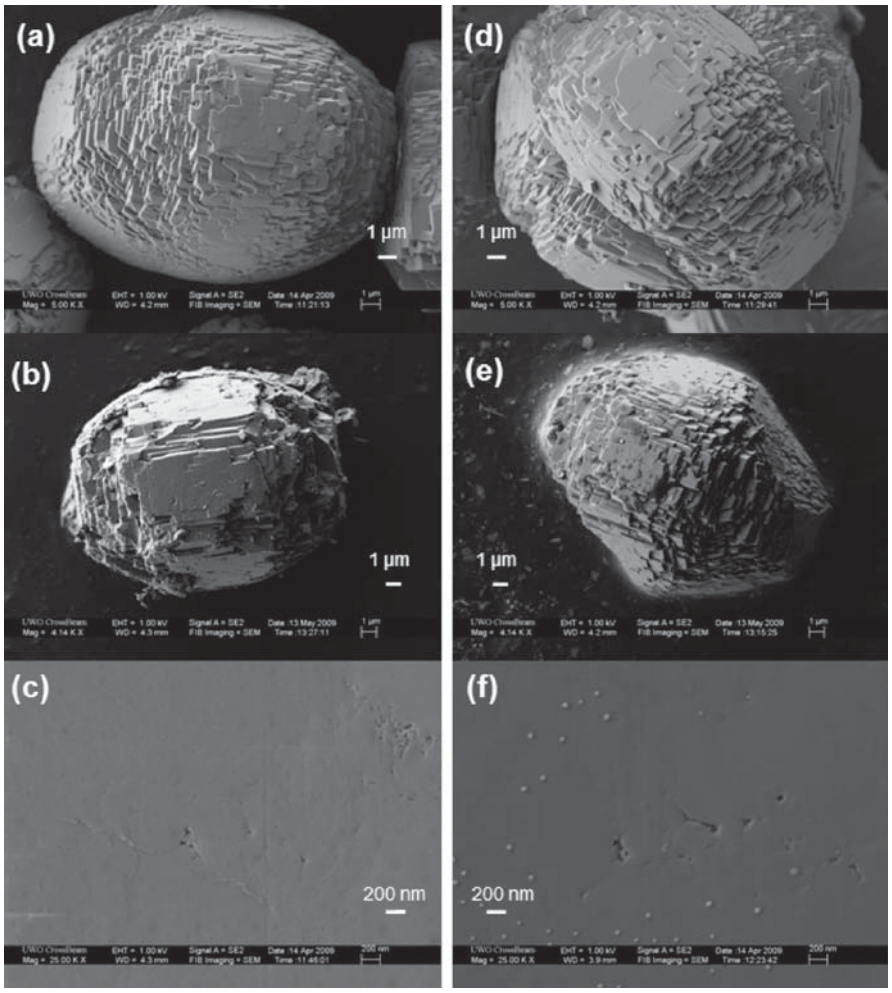

Figure 9. Scanning electron micrographs of the morphology of as-made Si-ZSM-5 (a) before compression, (b) recovered from 7.3 GPa, (c) recovered from 16.3 GPa, and calcined Si-ZSM-5 (d) before compression, (e) recovered from 2.7 GPa, and (f) recovered from 13.9 GPa (tiny balls on the surface are due to the contaminates from air).

Raman spectra of the recovered calcined Si-ZSM-5 samples from different high-pressure experiments are shown in Figure 8b. The spectrum of the sample recovered from 2.7 GPa looks similar to that of the same sample before compression, suggesting the PIA is almost reversible when the sample is treated at 2.7 GPa or less. The spectrum of the sample recovered from 3.4 GPa is quite different from that of the uncompressed sample, since all the zeolite peaks become very broad and weak, especially the initial strongest peak at 385 cm^{-1}, which now overlaps with the peaks due to amorphous silica as a featureless hump. These observations imply that the recovered sample is a mixture of an amorphous phase and the recovered ZSM-5. Therefore, the PIA is only partially reversible after the treatment at the maximum pressure of 3.4 GPa. The spectra of the samples recovered from 11.3 and 13.9 GPa are the same. Only the new bands due to the HDA silica are clearly visible. All the initial zeolite bands vanish, suggesting that the zeolite becomes completely amorphous after being compressed at the pressures above 11 GPa and the PIA is irreversible at this pressure. These results indicate that the formation of the HDA silica takes place at about 3 GPa for calcined Si-ZSM-5, and the PIA is reversible before the occurrence of the HDA silica. The conversion of the LDA to HDA silica finishes at about 11 GPa; above this pressure only the HDA silica exists in the system. The XRD results are consistent with those extracted from Raman spectra. The pattern of the calcined ZSM-5 recovered from compression to 2.8 GPa looks identical to that before the compression, whereas the pattern of the sample recovered from 13.0 GPa exhibits no reflection due to ZSM-5 (Figure S3). Overall, the PIA of the as-made Si-ZSM-5 is reversible in a wider pressure range (0−7 GPa) than that of the calcined one (0−3 GPa).

SEM was used to visualize the effect of pressure on sample's morphology. The SEM images in Figure 9 show the morphologies of the as-made and calcined Si-ZSM-5 before compression and recovered after treatment at different pressures. The individual as-made Si-ZSM-5 crystals have a near-ovate shape with dimensions close to 20 μm × 15 μm before compression. After being retrieved from 7.3 GPa, crystals similar to those before compression can be found in the recovered sample shown in Figure 9b, suggesting that the sample recrystallizes from the amorphous material. This confirms that the PIA is reversible at this pressure.

Upon releasing the sample from 16.3 GPa, no zeolite crystal can be seen (Figure 9c); only a large plate with flat surface forms inside the hole of the gasket, showing no crystal morphology. This suggests that the sample has totally lost its crystalline

structure and becomes an amorphous material. Thus, PIA is irreversible at this pressure. An amorphous material with a similar morphology has been found after treating zeolite Y at 8 GPa and then decompressing.[21] Before compression, the calcined Si-ZSM-5 crystals shown in Figure 9d look similar to those of the as-made Si-ZSM-5. After decompression from 2.7 GPa, Si-ZSM-5 recrystallizes (Figure 9e), indicating that the PIA is completely reversible at this pressure. For the sample recovered from 13.9 GPa (Figure 9f), all the initial zeolite crystals are fused into a large plate, suggesting that the sample has totally lost its crystalline structure.

CONCLUSIONS

As-made Si-ZSM-5 undergoes two successive phase transitions during the PIA process. The crystalline zeolite starts transforming to the LDA silica at around 3 GPa. Between 3 and 7 GPa, as-made Si-ZSM-5 and the LDA silica coexist. The amount of the LDA silica gradually increases with increasing pressure. In the LDA phase, the MFI topology is likely retained, but the long-range ordering is lost. For the sample treated at 7 GPa or lower, the PIA is completely reversible. The LDA phase starts evolving into the HDA silica at around 7 GPa. The conversion likely occurs via collapsing of the larger 10-MR channels to form the smaller rings (3- and 4-MRs), leading to a denser amorphous material. The HDA silica cannot transform back to the crystalline ZSM-5 upon decompression.

Calcined Si-ZSM-5 also experiences PIA and has two amorphous phases as well. The LDA silica starts forming at around 1.5 GPa and begins to evolve into the HDA silica at around 3 GPa. At this stage, the sample can still recrystallize back to ZSM-5 upon releasing pressure. Above 3 GPa, the LDA phase continues to transform to the HDA silica upon further compression. Above 11 GPa, only the HDA silica exists in the system and the PIA is irreversible.

Although both as-made and calcined Si-ZSM-5 undergo PIA, their threshold pressures of amorphization and polyamorphic transition are different. These pressures for calcined Si-ZSM-5 are much lower than those of as-made Si-ZSM-5. Calcined Si-ZSM-5 deforms much earlier than as-made Si-ZSM-5 under pressure. This is because calcined Si-ZSM-5 has no template molecules to reinforce the 10-MR channels. For both zeolites, the LDA phase can be transformed back to the original crystalline MFI structure. However, the pressure range for this reversible phase transition is much wider for as-made Si-ZSM-5 (0−7 GPa) than that for the calcined one (0−3 GPa), indicating that the TPA^+ cations also act as "organizing centers" to redirect the silica fragments with zeolite formwork signature to reform the MFI topology.[5]

ASSOCIATED CONTENT

Supporting Information. A table of Raman modes of the as-made Si-ZSM-5 sample containing TPA^+ cations, selected Raman spectra of the crystalline TPAB on compression and decompression, and powder XRD patterns of recovered calcined ZSM-5. This material is available free of charge via the Internet at http://pubs.acs.org.

ACKNOWLEDGMENT

Y.F. acknowledges experimental assistance from Z. Dong and S. Xie. Y.H. and Y.S. thank the Natural Science and Engineering Research Council of Canada for Discovery Grants. Funds from the Canada Research Chair program (Y.H.) and Early Researcher Award from the Ontario Ministry of Research and Innovation (Y.S.) are also gratefully acknowledged. The X-ray work was performed at HPCAT (Sector 16), APS, ANL. HPCAT is supported by CIW, CDAC, UNLV, and LLNL through funding from DOE-NNSA, DOE-BES, and NSF. APS is supported by DOE-BES, under Contract No. DE-AC02-06CH11357.

REFERENCES

(1) Dyer, A. *An Introduction to Zeolite Molecular Sieves*; John Wiley & Sons: Chichester, New York, 1988.
(2) Xu, R.; Pang, W.; Yu, J.; Huo, Q.; Chen, J. *Chemistry of Zeolites and Related Porous Materials: Synthesis and Structure*; Wiley-VCH: Weinheim, Germany, 2007.
(3) Bish, D. L.; Carey, J. W. *Rev. Mineral. Geochem.* **2001**, *45*, 403–452.
(4) Hazen, R. M. *Science* **1983**, *219*, 1065–7.
(5) Tse, J. S.; Klug, D. D.; Ripmeester, J. A.; Desgrenlers, S.; Lagarec, K. *Nature* **1994**, *369*, 724–7.
(6) Lee, Y.; Hriljac, J. A.; Vogt, T.; Parise, J. B.; Edmondson, M. J.; Anderson, P. A.; Corbin, D. R.; Nagai, T. *J. Am. Chem. Soc.* **2001**, *123*, 8418–8419.
(7) Lee, Y.; Vogt, T.; Hriljac, J. A.; Parise, J. B.; Hanson, J. C.; Kim, S. J. *Nature* **2002**, *420*, 485–489.
(8) Havenga, E. A.; Huang, Y.; Secco, R. A. *Mater. Res. Bull.* **2003**, *38*, 381–387.
(9) Secco, R. A.; Goryainov, S. V.; Huang, Y. *Phys. Status Solidi B* **2005**, *242*, R73–R75.
(10) Greaves, G. N.; Meneau, F.; Kargl, F.; Ward, D.; Holliman, P.; Albergamo, F. *J. Phys.: Condens. Matter* **2007**, *19*, 415102/1–415102/17.
(11) Ori, S.; Quartieri, S.; Vezzalini, G.; Dmitriev, V. *Am. Mineral.* **2008**, *93*, 53–62.
(12) Arletti, R.; Ferro, O.; Quartieri, S.; Sani, A.; Tabacchi, G.; Vezzalini, G. *Am. Mineral.* **2003**, *88*, 1416–1422.
(13) Hriljac, J. A. *Crystallogr. Rev.* **2006**, *12*, 181–193.
(14) Hazen, R. M.; Finger, L. W. *Phase Transitions* **1979**, *1*, 1–22.
(15) Lee, Y.; Lee, H. H.; Lee, D. R.; Shin, T. J.; Choi, J.-Y.; Kao, C.-C. *J. Am. Chem. Soc.* **2007**, *129*, 4888–4889.
(16) Secco, R. A.; Rutter, M.; Huang, Y. *Tech. Phys.* **2000**, *45*, 1447–1451.
(17) Huang, Y.; Havenga, E. A. *Chem. Phys. Lett.* **2001**, *345*, 65–71.
(18) Mishima, O.; Calvert, L. D.; Whalley, E. *Nature* **1984**, *310*, 393–5.
(19) Rutter, M. D.; Uchida, T.; Secco, R. A.; Huang, Y.; Wang, Y. *J. Phys. Chem. Solids* **2001**, *62*, 599–606.
(20) Gulin-Gonzalez, J.; Suffritti, G. B. *Microporous Mesoporous Mater.* **2004**, *69*, 127–134.
(21) Greaves, G. N.; Meneau, F.; Sapelkin, A.; Colyer, L. M.; ap Gwynn, I.; Wade, S.; Sankar, G. *Nat. Mater.* **2003**, *2*, 622–629.
(22) Sharma, S. M.; Sikka, S. K. *Prog. Mater. Sci.* **1996**, *40*, 1–77.
(23) Gulin Gonzalez, J.; Dorta-Urra, A.; Demontis, P.; Suffritti, G. B. *Microporous Mesoporous Mater.* **2009**, *123*, 30–38.
(24) Zhang, J.; Zhao, Y.; Xu, H.; Zelinskas, M. V.; Wang, L.; Wang, Y.; Uchida, T. *Chem. Mater.* **2005**, *17*, 2817–2824.
(25) Belitskii, I. A.; Fursenko, B. A.; Gabuda, S. P.; Kholdeev, O. V.; Seretkin, Y. V. *Phys. Chem. Miner* **1992**, *18*, 497–505.
(26) Readman, J. E.; Forster, P. M.; Chapman, K. W.; Chupas, P. J.; Parise, J. B.; Hriljac, J. A. *J. Chem. Soc., Chem. Commun.* **2009**, 3383–3385.
(27) Greaves, N.; Meneau, F. *J. Phys.: Condens. Matter* **2004**, *16*, S3459–S3472.
(28) Greaves, G. N.; Meneau, F.; Majerus, O.; Jones, D. G.; Taylor, J. *Science* **2005**, *308*, 1299–1302.
(29) Wilding, M. C.; Wilson, M.; McMillan, P. F. *Chem. Soc. Rev.* **2006**, *35*, 964–986.
(30) Peral, I.; Iniguez, J. *Phys. Rev. Lett.* **2006**, *97*, 225502/1–225502/4.
(31) Cohen, M. H.; Iniguez, J.; Neaton, J. B. *J. Non-Cryst. Solids* **2002**, *307−310*, 602–612.

(32) Fois, E.; Gamba, A.; Tabacchi, G.; Arletti, R.; Quartieri, S.; Vezzalini, G. *Am. Mineral.* **2005**, *90*, 28–35.
(33) Tabak, S. A.; Yurchak, S. *Catal. Today* **1990**, *6*, 307–27.
(34) Degnan, T. F.; Chitnis, G. K.; Schipper, P. H. *Microporous Mesoporous Mater.* **2000**, *35*−*36*, 245–252.
(35) Bosselet, F.; Sacerdote, M.; Bouix, J.; Mentzen, B. F. *Mater. Res. Bull.* **1990**, *25*, 443–50.
(36) Oehrman, O.; Hedlund, J. *Microporous Mesoporous Mater.* **2006**, *91*, 312–320.
(37) Zou, X.; Zhu, G.; Guo, H.; Jing, X.; Xu, D.; Qiu, S. *Microporous Mesoporous Mater.* **2009**, *124*, 70–75.
(38) Cundy, C. S.; Cox, P. A. *Microporous Mesoporous Mater.* **2005**, *82*, 1–78.
(39) Olson, D. H.; Kokotailo, G. T.; Lawton, S. L.; Meier, W. M. *J. Phys. Chem.* **1981**, *85*, 2238–43.
(40) Van Koningsveld, H.; Van Bekkum, H.; Jansen, J. C. *Acta Crystallogr., Sect. B: Struct. Sci.* **1987**, *B43*, 127–32.
(41) Liu, X.; Su, W.; Wang, Y.; Zhao, X. *J. Chem. Soc., Chem. Commun.* **1992**, 902–3.
(42) Haines, J.; Levelut, C.; Isambert, A.; Hebert, P.; Kohara, S.; Keen, D. A.; Hammouda, T.; Andrault, D. *J. Am. Chem. Soc.* **2009**, *131*, 12333–12338.
(43) Haines, J.; Cambon, O.; Levelut, C.; Santoro, M.; Gorelli, F.; Garbarino, G. *J. Am. Chem. Soc.* **2010**, *132*, 8860–8861.
(44) Robson, H. Collection of Verified Zeolite Synthesis. *Microporous Mesoporous Mater.* **1998**, *22*, 628.
(45) Colligan, M.; Forster, P. M.; Cheetham, A. K.; Lee, Y.; Vogt, T.; Hriljac, J. A. *J. Am. Chem. Soc.* **2004**, *126*, 12015–12022.
(46) Gatta, G. D.; Comodi, P.; Zanazzi, P. F.; Ballaran, T. B. *Am. Mineral.* **2005**, *90*, 645–652.
(47) Bartlett, J. R.; Cooney, R. P.; Bibby, D. M. *Stud. Surf. Sci. Catal.* **1988**, *36*, 609–14.
(48) Bremard, C.; Laureyns, J.; Patarin, J. *J. Raman Spectrosc.* **1996**, *27*, 439–445.
(49) Hemley, R. J.; Mao, H. K.; Bell, P. M.; Mysen, B. O. *Phys. Rev. Lett.* **1986**, *57*, 747–50.
(50) Champagnon, B.; Martinet, C.; Boudeulle, M.; Vouagner, D.; Coussa, C.; Deschamps, T.; Grosvalet, L. *J. Non-Cryst. Solids* **2008**, *354*, 569–573.
(51) Grimsditch, M. *Phys. Rev. Lett.* **1984**, *52*, 2379–81.
(52) Sharma, S. K.; Mammone, J. F.; Nicol, M. F. *Nature* **1981**, *292*, 140–1.
(53) Galeener, F. L. *Solid State Commun.* **1982**, *44*, 1037–40.
(54) Xu, Z.; Huang, Y.; Butler, I. S. *Vib. Spectrosc.* **2009**, *51*, 251–254.
(55) Dutta, P. K.; Puri, M. *J. Phys. Chem.* **1987**, *91*, 4329–33.
(56) Bock, J.; Su, G.-J. *J. Am. Ceram. Soc.* **1970**, *53*, 69–73.
(57) Pasquarello, A.; Car, R. *Phys. Rev. Lett.* **1998**, *80*, 5145–5147.
(58) Daniel, I.; Gillet, P.; McMillan, P. F.; Wolf, G.; Verhelst, M. A. *J. Geophys. Res., [Solid Earth]* **1997**, *102*, 10313–10325.